Available online at www.sciencedirect.com

ScienceDirect

Procedia Manufacturing 47 (2020) 148–153

Procedia MANUFACTURING

www.elsevier.com/locate/procedia

23rd International Conference on Material Forming (ESAFORM 2020)

Experimental Measurement of the Resistant Load in Injection Pultrusion Processes

Fausto Tucci[a,*], Vitantonio Esperto[b], Felice Rubino[b], Pierpaolo Carlone[a]

[a] *Department of Industrial Engineering, University of Salerno, 132, Via Giovanni Paolo II, Fisciano 84084, Italy*
[b] *Department of Chemical, Materials and Industrial Production Engineering, University of Naples "Federico II", 80, Piazzale Tecchio, Napoli, Italy.*

* Corresponding author. Tel.: +39-089964320. *E-mail address:* ftucci@unisa.it

Abstract

Injection pultrusion (IP) process is a manufacturing technique for producing advanced fiber reinforced polymers having constant cross-section. Unlike the traditional pultrusion process, in which fibers are impregnated passing through an open bath of liquid resin, in IP the uncured polymer is directly injected within the advancing reinforcement in a close chamber generally connected to the die. This paper investigates the resistant forces evolution in IP process at different pulling speeds. Resistant loads are mainly due to the interaction between the advancing material and the die cavity walls, inducing residual stress and, eventually, internal defects. These loads are typically classified in three main contributes, namely fiber collimation, viscous drag and solid friction. The latter two are directly related to the resin degree of cure, and, therefore, the overall resistant load is dramatically sensitive to the changes in operative parameters. In this paper, the resistant force acting along the die cavity has been measured using a dedicated experimental setup. Measurements were performed during the pultrusion of glass-reinforced polyester with different pulling speeds to evidence the variations in resistant load as a function of the process velocity.

Keywords: Injection pultrusion; Fiber reinforced polymer; Pulling force; Viscous drag; Degree of cure.

1. Introduction

Advanced fiber reinforced polymers are attracting growing attention due to their physical and mechanical properties [1]. In particular, out-of-autoclave processes significantly reduce the tooling cost and the energy consumption at the manufacturing stage [2–4]. Among out-of-autoclave processes, pultrusion technique is gaining particular interest, due to the enhanced mechanical performances achievable and to the low costs [5]. Pultrusion is a technique to produce constant cross-section fiber reinforced polymers [6–8]. Pultruded profiles are employed in structural application in which high longitudinal stiffness and strength are required along a peculiar direction. Indeed, as a direct consequence of the used manufacturing process, these products exhibit significant anisotropy, due to the disposition and the direction of the fibrous reinforcement [9].

In injection pultrusion lines, the fibrous reinforcement, stored as roving bobbins or fibers fabrics, is driven through a preforming system toward the curing-forming tools. This equipment is composed by a tapered injection chamber and a straight heated die. Impregnation occurs within a closed chamber, in which resin is injected through the fibrous reinforcement by means of nozzles, avoiding any exposure of the liquid polymer with the external working environment [10]. The fibers drag the resin through the straight cavity of a steel die. The die is heated by electrical platens, controlled in temperature, to provide the resin with the thermal energy necessary to activate the polymerization reaction. The continuous process is moved by a pulling system located at the end of the line [11].

The choice of the process parameters affects directly the curing cycle of the resin, and, therefore, the quality of the final

10.1016/j.promfg.2020.04.157

product [12]. Typical defects occurring in pultruded profiles are related to air embedding [13], geometrical distortions [6,14,15], delamination or interlayer cracks [16]. The pulling force plays a key role in this regard [17].

The present paper deals with the experimental measurement of the resistant load profile along the cavity of an injection pultrusion line. Measurements have been repeated setting two different speeds and without variations in the imposed temperature. The achieved load profiles have been discussed accounting for the rheology behavior of the resin during the cure reaction.

Nomenclature

α	Degree of cure [/]
T	Temperature [K]
t	Time [s]
x	Distance from the chamber inlet [mm]
R	Universal gas constant = 8.3145 [J mol^{-1} K^{-1}]
v_{pull}	Pulling speed [mm s^{-1}]
A_1	Frequency factor [s^{-1}]
E_1	Activation energy [J mol^{-1}]
m	First kinetic exponent [/]
n	Second kinetic exponent [/]
a_η	Pre-exponential viscosity coefficient [Pa s]
b_η	Second viscosity coefficient [J mol^{-1}]
k_1	Third viscosity coefficient [/]
k_2	Fourth viscosity coefficient [/]
$Q(x)$	Cumulated resistant force [N]
$F(x)$	Local resistant force [N mm^{-1}]
x_f	Die outlet position = 1090 [mm]
x_c	Cut section position [mm]
t_c	Cutting instant [s]

2. Materials and Methods

The experimental tests were conducted using a laboratory scale injection pultrusion system. The pultrusion line used in the present experimental analysis is depicted in Fig. 1. The curing-forming tool is composed of a tapered injection chamber 190 mm long, bolted on the heating die, presenting a 900 mm long straight cavity. The employed resin system is based on ortophtalic polyester (ESI resin GP med OT, produced by Euroresins ltd.) and on specific additives to strongly activate the reaction at high temperature. The reinforcement is constituted by 18 rovings of E-glass (tex number 2400). According to the shape of the cavity, the nominal diameter of the pultruded profile is 6 mm. Taking into account the amount of reinforcement involved and the cross-section of the produced FRP, the fiber volume fraction is expected to be equal to 59%. The injection system (fig. 2) drives the uncured liquid resin toward a tapered chamber (fig. 3), converging to the die geometry. Within the tapered cavity, the resin impregnates the advancing fibrous reinforcement. Three pairs of thermo-electric heating plates are mechanically fixed on the die top and bottom surfaces. Each couple of heaters is monitored and controlled in temperature using J-type thermocouples and a regulation system. The temperatures of the first, the second and the third couples of heating plates are respectively set equal to 80°C, 110°C and 130°C, in order to provide to the polymeric resin the thermal cycle necessary to achieve a satisfactory cure. Each of the thermal plates covers a rectangular surface 280 [mm] long and 100 [mm] wide. A cooling system prevents the increase of the temperature at the entrance of the die, and, therefore, of the advancing material in the earliest region of the straight cavity. The purpose of the cooling system is to avoid premature local polymerizations which can lead to defects or, in the worst case, to the stacking of the material in the die and, as a consequence, the interruption of the continue production. The cooling fluid is moved by a hydraulic centrifugal pump and cooled down using a forced convection heat exchanger, which uses air at room temperature. The cooling fluid flows through two channels milled within the steel die, at a distance of 50 [mm] from the straight cavity inlet in longitudinal direction. The advancing velocity was controlled by a caterpillar located at the end of the line. In the present work, two pulling speeds were investigated, namely 100 and 200 [mm/min].

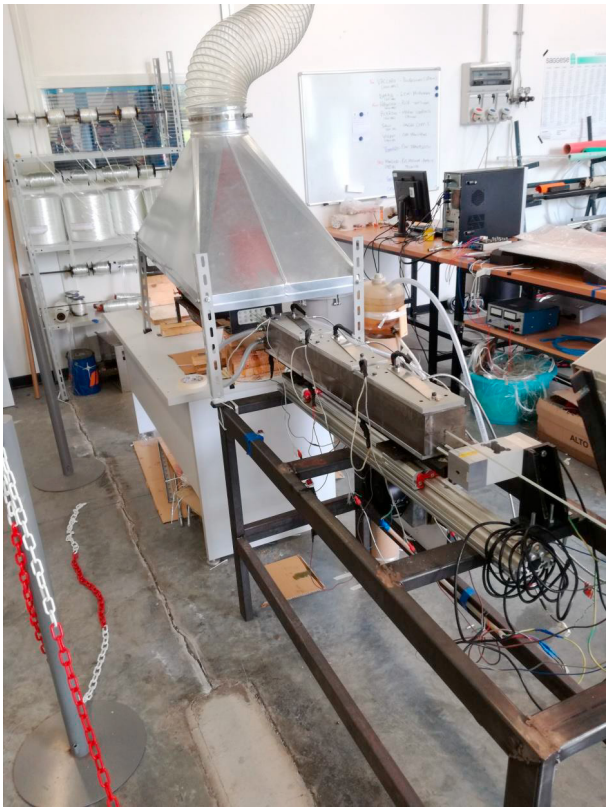

Fig. 1. Injection pultrusion line.

During the process, the temperature of the advancing material has been measured using a K-type travelling thermocouple, adhesively connected to the advancing fibers. The position of the bulb has been evaluated taking into account the velocity of the process.

Fig. 2. Resin injection system.

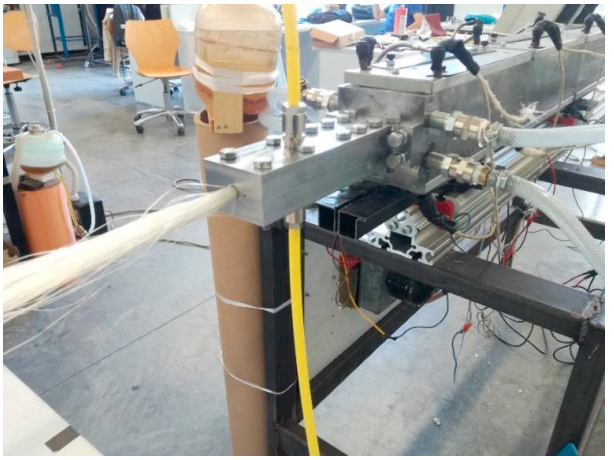

Fig. 3. Tapered injection chamber.

The kinetic of the resin was assessed by means of differential scanning calorimetric analysis, performed setting dynamic ramps of 10, 15, 20, 25, 30 [K/min]. Equation 1 describes the cure reaction evolution of the resin adopted in this work.

$$\frac{d\alpha}{dt} = A_1 exp\left(\frac{E_1}{R\,T}\right)\alpha^m(1-\alpha)^n \quad (1)$$

The parameter A_1 is the pre-exponential factors, also known as frequency factor, the parameter E_1 is the activation energie, R is the universal constant of the gas, m and n are the kinetic exponents of the reaction. The degree of cure α has been estimated hypnotizing that the cure is null at the die inlet. The resin viscosity has been predicted considering the behavior described in eq. 2 [18].

$$\eta = a_\eta exp\left(\frac{b_\eta}{R\,T} + k\alpha\right) \quad (2)$$

The values of the coefficients of equations 1 and 2 are reported in table 1.

Table 1. Kinetic and rheology coefficients of the resin.

Symbol	Value	Unit
A_1	7.5581 E+9	[s^{-1}]
E_1	8.2727 E+4	[J mol^{-1}]
m	6.3 E-1	[/]
n	1.847	[/]
a_η	1.08 E-6	[Pa s]
b_η	4.0147 E+4	[J mol^{-1}]
k	8.339 E+1	[/]

Fig. 4 describes the system implemented to measure the force along the pulling direction and opposing the movement of the workpiece. The die, free to slide on a longitudinal guide impact on a load cell fixed on the limit of the guide. The load cell is a compressive button connected to a signal amplifier and an *ArduinoUno* board, connected to a computer and interrogated by a code implemented using the *LabView* suite.

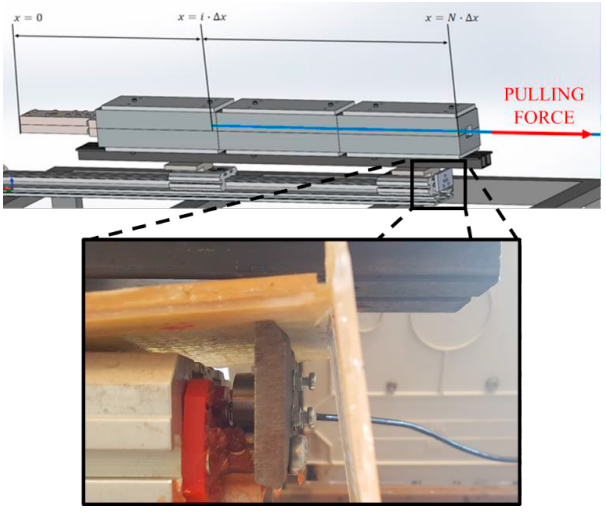

Fig. 4. Pulling force measurement system.

The load cell has been calibrated before each performed tests, using blocks of known weight, connected to the die using an opportune system of wire and pulley.

Due to the system setting and disposition, during the stationary pultrusion process, the load cell acquires the resistant force produced by the contact between the advancing composite and the whole cavity. In order to measure the profile of the resistance to the pull $F(x)$ along the cavity, during a stationary stable pultrusion process, the advancing fiber were cut before entering in the inlet of the injection chamber. The cut section position $x_c(t)$ is evaluated as a function of the time accounting for the time instant in which it pass through the chamber inlet and for the constant pulling speed. Using this technique, the load cell detects the value of the total resistance $Q(x)$, arising between the position of the advancing cut section $x_c(t)$ and the die outlet x_f, as described in eq. 3 [19].

$$Q(x) = \int_{x_c(t)}^{x_f} F(x)\,dx \tag{3}$$

Therefore, the local force $F(x)$ can be estimated as follows.

$$F(x) = -\frac{dQ(x)}{dx} \tag{4}$$

The position of the cut section $x_c(t)$ is computed accounting for the pulling speed v_{pull} and for the time delay from the cutting instant t_c, as described in eq. 5.

$$x_c(t) = v_{pull}(t - t_c) \tag{5}$$

3. Results and discussion

Fig. 5 shows the data collected during the two experimental tests.

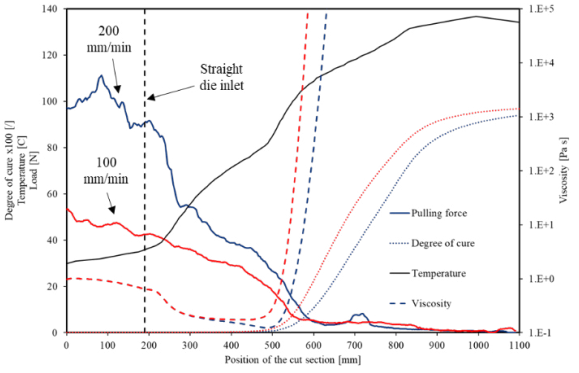

Fig. 5. Experimentally measured load and temperature profiles; numerically evaluated degree of cure and viscosity evolutions.

The measured or computed data have been plotted against the position of the cut section along the chamber and die cavity. Blue lines refer to the process performed at 200 mm/min, while the red lines are relative to the process performed at 100 mm/min. The black dashed line separates the tapered injection chamber (the earliest 190 mm) from the straight die (last 900 mm). The solid thick lines are the resistant forces acquired by the load cell, the dashed lines represent the viscosity evolution and the pointed curves are the degree of cure profiles in the two cases.

The differences in temperature result negligible. Reinforcing fibers enter in the system at room temperature. Along the injection chamber, it can be noticed a slight thermal gradient. Indeed, upstream the cooling system, located at a distance of 240 mm from the chamber inlet, the heat flow is absorbed and dissipated by the cooling system. Downstream the cooling system, the material temperature increases due to the heating plates. At a distance of about 700 mm, the material temperature overcomes the temperature of heating plates. This phenomenon is due to the exothermal nature of cure reaction: the thermal energy produced by the resin is proportional to the cure rate [20]. The polymerization of thermosetting resin is an irreversible reaction; therefore, the cure profile is always increasing. The degree of cure is null in the injection chamber and in the first 300 mm of the straight die. At about 500 mm from the chamber inlet, the cure reaction is activated and the degree of cure starts increasing. The reaction is initially very fast and presents high cure rate. When the degree of cure approaches to the unit value, the cure gradient gradually decreases, until it reaches a *plateau*. Both the curves show the activation of the curing process approximately at the same position. After activation, the cure in the higher speed case (blue line) presents a delay, if compared to the lower speed case (red line). At the die outlet, the degree of cure is 97% in the slow case and 94% in the fast case. The dissimilarities between the two reactions are due to the different thermal cycles imposed to the resin. Indeed, in the fast case, the crossing time is the half of the short case. On the other hand, the faster the heating cycle is, the sharper the cure reaction is [21]. Therefore, the cure rate in the fast case is remarkably higher than the one in the slow case. The resin viscosity has a variation of several order of magnitude during the process. Therefore, in order to appreciate the rheological evolution of the resin, the viscosity curves are plotted on logarithm axis. Viscosity depends on cure and temperature, accordingly to eq. 2. Unreacted resin at room temperature exhibits a viscosity of about 1 [Pa s]. Upstream the resin activation, only the temperature effects influence the resin. In the earliest 240 [mm], the viscosity slightly decreases. Once overcome the cooling system the resin viscosity shows a marked decrease, up to about 0.1 [Pa s]. At the cure activation, viscosity curves reach their minimum. During polymerization the liquid resin turn to the gel state and then to a glassy state. These transformations imply a sharp rise in viscosity. The two viscosity curves, as well as the degree of cure curves, are not overlapping: in the fast case, the viscosity curve is delayed with respect to the slow case of about 30 [mm]. Moreover, in the fast case, viscosity reaches a lower value, due to the delay in cure reaction and to the effect of the thermal ramp velocity [22].

To analyse the resistant load curves it should be noticed that higher decrease in the cumulative load curve means higher local load at that coordinate, accordingly to equation 4. The resistant load curves are expected to decrease along the entire die, since the contact area between the advancing material and the cavity wall decrease as the cut section advances. The

resistant load arising within the die can be considered as the sum of three contributes: the bulk compaction force, the viscous drag and the solid friction [17]. The bulk compaction force related to the compaction of the fibrous reinforcement within the die cavity. The viscous drag arises before gel transition whereas the resin presents a viscous liquid behaviour. The solid friction is related to the contact between the wall and the advancing material after resin glass transition. In the load curves depicted in figure 3 the bulk compaction can be appreciated in the injection chamber zone, where the load is slightly decreasing. The tapered cavity transversally compress the advancing reinforcement. When the cut section crosses the first 100 mm of the injection chamber the width of the cavity, the reinforcement presents a low compaction. Due to this aspect and to the presence of the cut end, the fibers are free to move; therefore, the evaluation of the interaction between the wet fibers and the chamber cavity produces, in this short section, non-reliable measures. It can be appreciated that in the straight cavity, where the material is strongly constrained, the load curves do not present noise and unphysical oscillations. In the injection chamber, the presence of the liquid resin implies also the action of viscous drag. At this stage, beside the low variation in viscosity, other factors, namely the geometrical narrowing of the cavity and the high mobility of the fiber reinforcement, influence the viscous resistance. The viscous drag can be observed between the straight cavity inlet and the activation of the cure reaction. At a distance of 240 mm from the chamber inlet, temperature sharply increase and viscosity remarkably drops. Due to this drop, the viscous drag gradually decreases. At the cure activation, the resin viscosity and the viscous drag sharply increases: a drop in the resistant load can be appreciated between 450 and 600 [mm] from the injection chamber inlet. The glass transition is detected by the change in the slope of the load curves. In the last 500 mm of the die the cumulate resistant load linearly decreases. In this final zone, the contact between advancing material and die has a solid frictional nature. It is worth to notice that in the fast case, the slope of the cumulative load curve in the “viscous zone” is twice higher than the slope in the slow case. Indeed, accordingly to equation 4, the slope is equal to the local interaction between the advancing material and the cavity wall. The viscous interaction linearly depends on the velocity, and, in the fast case, the pulling speed is exactly the double of the slow case one. The delay in cure activation implies a delay in the gel and glass transitions. Therefore, in the fast case, the load curve drop due to these transitions occurs about 30 mm downstream the slow case drop. Frictional resistance is almost negligible if compared to the viscous drag and the bulk compaction. This is mainly due to the chemical shrinkage of the resin, which decreases the contact pressure between the solid profile and the cavity wall.

4. Conclusions

The present manuscript investigates the loads resistant to the pulling force arising within the curing-forming die in injection pultrusion processes. The resistant forces have been evaluated accounting for the chemical evolution of the resin and, therefore, for its the variations in its mechanical and physical properties. The discussion evidence the following conclusions:

- The heating temperatures and the pulling speed significantly affect the resistant loads;
- Cure kinetic and viscosity evolution of the resin play a key role in the interaction between the advancing impregnated fibers and the cavity walls;
- In the investigated process, the most of the resistance to the pulling force is related to the viscous drag, which results remarkably higher than the bulk compaction and the solid friction.

References

[1] Aleksendrić D, Bellini C, Carlone P, Ćirović V, Rubino F, Sorrentino L. Neural-fuzzy optimization of thick composites curing process. Mater Manuf Process 2019;34:262–73.
[2] Carlone P, Rubino F, Paradiso V, Tucci F. Multi-scale modeling and online monitoring of resin flow through dual-scale textiles in liquid composite molding processes. Int J Adv Manuf Technol 2018.
[3] Rubino F, Carlone P. A semi-analytical model to predict infusion time and reinforcement thickness in VARTM and SCRIMP processes. Polymers (Basel) 2018;11.
[4] Carlone P, Aleksendrić D, Rubino F, Ćirović V. Artificial Neural Networks in Advanced Thermoset Matrix Composite Manufacturing. Lect. Notes Mech. Eng., vol. 2, Springer International Publishing; 2018, p. 194–210.
[5] Nickels L. The future of pultrusion. Reinf Plast 2019;63:132–5.
[6] Baran I, Akkerman R, Hattel JH. Modelling the pultrusion process of an industrial L-shaped composite profile. Compos Struct 2014;118:37–48.
[7] Carlone P, Palazzo GS, Pasquino R. Pultrusion manufacturing process development by computational modelling and methods. Math Comput Model 2006;44:701–9.
[8] Carlone P, Palazzo GS, Pasquino R. Pultrusion manufacturing process development: Cure optimization by hybrid computational methods. Comput Math with Appl 2007;53:1464–71.
[9] Haj-Ali R, Kilic H. Nonlinear behavior of pultruded FRP composites. Compos Part BEngineering 2002;33.
[10] Tucci F, Rubino F, Carlone P. Strain and temperature measurement in pultrusion processes by fiber Bragg grating sensors. AIP Conf. Proc., vol. 1960, 2018.
[11] Starr TF. Pultrusion for engineers. 2000. doi:10.1533/9781855738881.97.
[12] Paciornik S, Martinho F., de Mauricio MH., d’Almeida JR. Analysis of the mechanical behavior and characterization of pultruded glass fiber–resin matrix composites. Compos Sci Technol 2003;63:295–304.
[13] Park JY, Zureick A-H. Effect of filler and void content on mechanical properties of pultruded composite materials under shear loading. Polym Compos 2005;26:181–92.
[14] Bellini C, Sorrentino L, Polini W, Corrado A. Spring-in analysis of CFRP thin laminates: numerical and experimental results. Compos Struct 2017;173:17–24.
[15] Safonov AA, Konstantinov AY. Mathematical simulation of residual deformation of complex composite profiles during pultrusion. Int. SAMPE Tech. Conf., vol. 2015- Janua, Soc. for the Advancement of Material and Process Engineering; 2015.
[16] Baran I, Straumit I, Shishkina O, Lomov SV. X-ray computed tomography characterization of manufacturing induced defects in a glass/polyester pultruded profile. Compos Struct 2018;195:74–82.
[17] Safonov AA, Carlone P, Akhatov I. Mathematical simulation of pultrusion processes: A review. Compos Struct 2018;184.
[18] Shanku R, Vaughan JG, Roux JA. Rheological Characteristics and Cure Kinetics of EPON 862 / W Epoxy Used in Pultrusion Measurements 1997;16:297–311.
[19] Tucci F, Rubino F, Esperto V, Carlone P. Integrated modeling of injection pultrusion. AIP Conf Proc 2019;2113.
[20] Tucci F, Rubino F, Paradiso V, Carlone P, Valente R. Modelling and simulation of cure in pultrusion processes. AIP Conf. Proc., vol. 1896, 2017.
[21] Hardis R, Jessop JLP, Peters FE, Kessler MR. Cure kinetics characterization and monitoring of an epoxy resin using DSC, Raman spectroscopy, and DEA. Compos Part A Appl Sci Manuf 2013;49:100–8.

[22] Liang G, Chandrashekhara K. Cure kinetics and rheology characterization of soy-based epoxy resin system. J Appl Polym Sci 2006;102:3168–80.